Signature of anyonic statistics in the integer quantum Hall regime

P. Glidic,[1] I. Petkovic,[1,*] C. Piquard,[1] A. Aassime,[1] A. Cavanna,[1] Y. Jin,[1]
U. Gennser,[1] C. Mora,[2] D. Kovrizhin,[3] A. Anthore,[1,4] and F. Pierre[1,†]

[1] *Université Paris-Saclay, CNRS, Centre de Nanosciences et de Nanotechnologies, 91120, Palaiseau, France*
[2] *Université Paris Cité, CNRS, Laboratoire Matériaux et Phénomènes Quantiques, 75013 Paris, France*
[3] *LPTM, CY Cergy Paris Universite, UMR CNRS 8089, Pontoise 95032 Cergy-Pontoise Cedex, France*
[4] *Université Paris Cité, CNRS, Centre de Nanosciences et de Nanotechnologies, F-91120, Palaiseau, France*

arXiv: 2401.06069

Qianhui Xu 2024.02.27

- Probe of anionic exchange statistics

1. Interferometry: anyons along the edge move around those in the bulk, and acquire a braiding (double exchange) phase.
2. Quantum point contact (QPC)

$\nu = 2$ Two co-propagating edge channels (Interacting fermionic edge states) $\xrightarrow[\text{Bosonization}]{\text{Chiral Luttinger liquid}}$ Two free edge magnetoplasmon (EMP) modes

EMP mode:

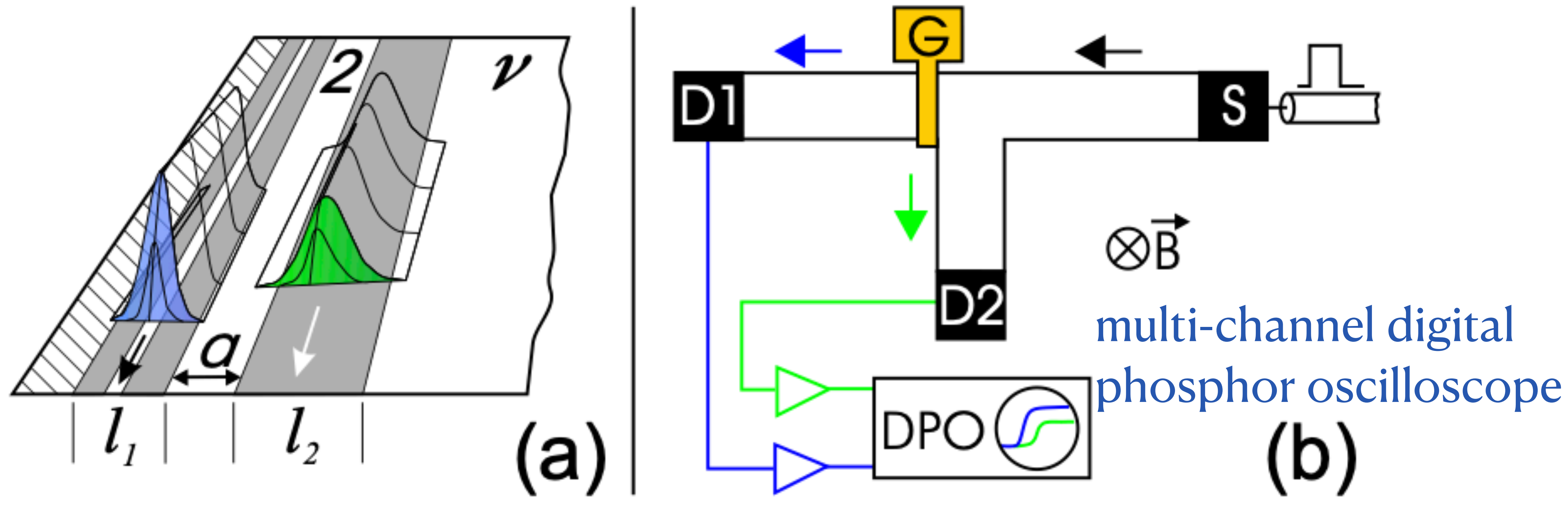

FIGURE 1. (a) Schematic view of two modes of EMP's decoupled by an incompressible strip with filling factor $\nu = 2$. Compressible strips are shown as grey areas, incompressible liquids as white areas, and the hatched region represents a depleted semiconductor at the mesa edge. (b) Sketch of experimental setup. The metallic top gate which covers the whole area of the sample is omitted for clarity.

AIP Conference Proceedings 772, 573 (2005); doi: 10.1063/1.1994237

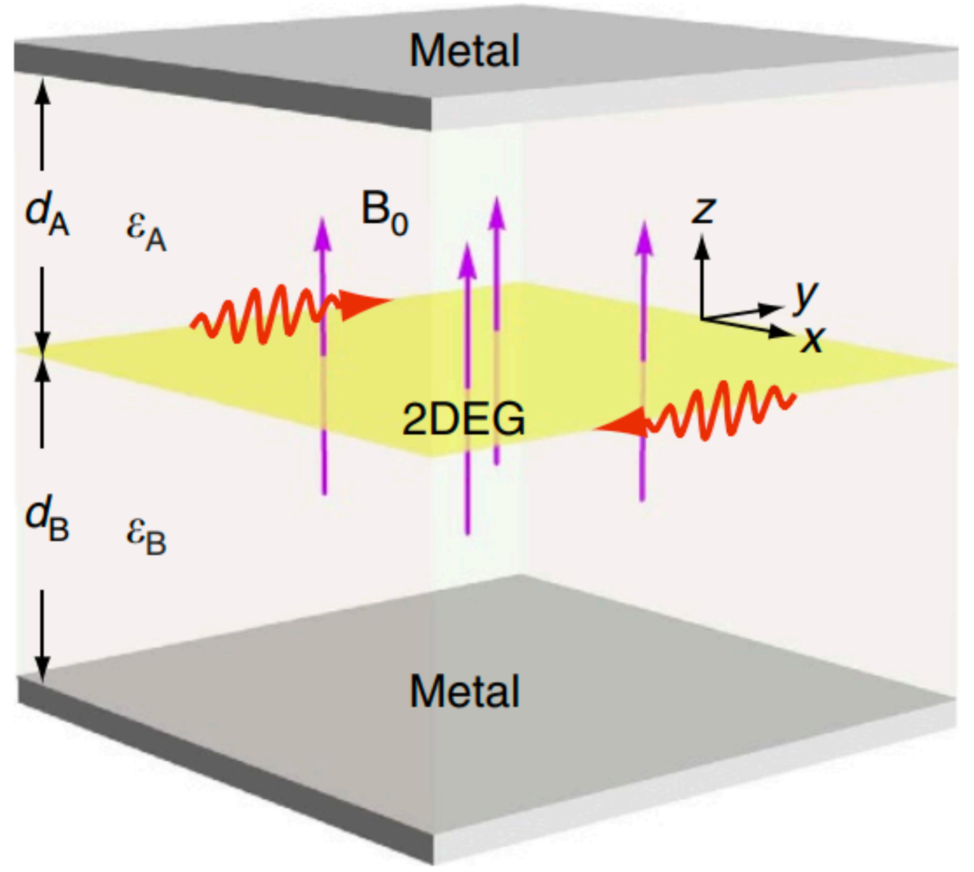

Plasmon: bosonic excitations.

collective motion of electron–hole pairs in a Coulomb interaction electron gas. Macroscopically it appears as coherent electron-density oscillations.

two wave packets of edge excitations moving with different velocities near the sample boundary.

G remains unbiased ($V = 0$ mV): the local filling factor g under the gate is equal to the bulk value ν and all edge channels (EC's) are transmitted to D1. A negative voltage V< 0: some fraction of the signal is deflected to D2. Setting $g = 2$ under the gate G we can measure the contribution of each Landau level by different drain contacts. The two outer EC's are transmitted to D1 and the innermost EC is deflected to D2.

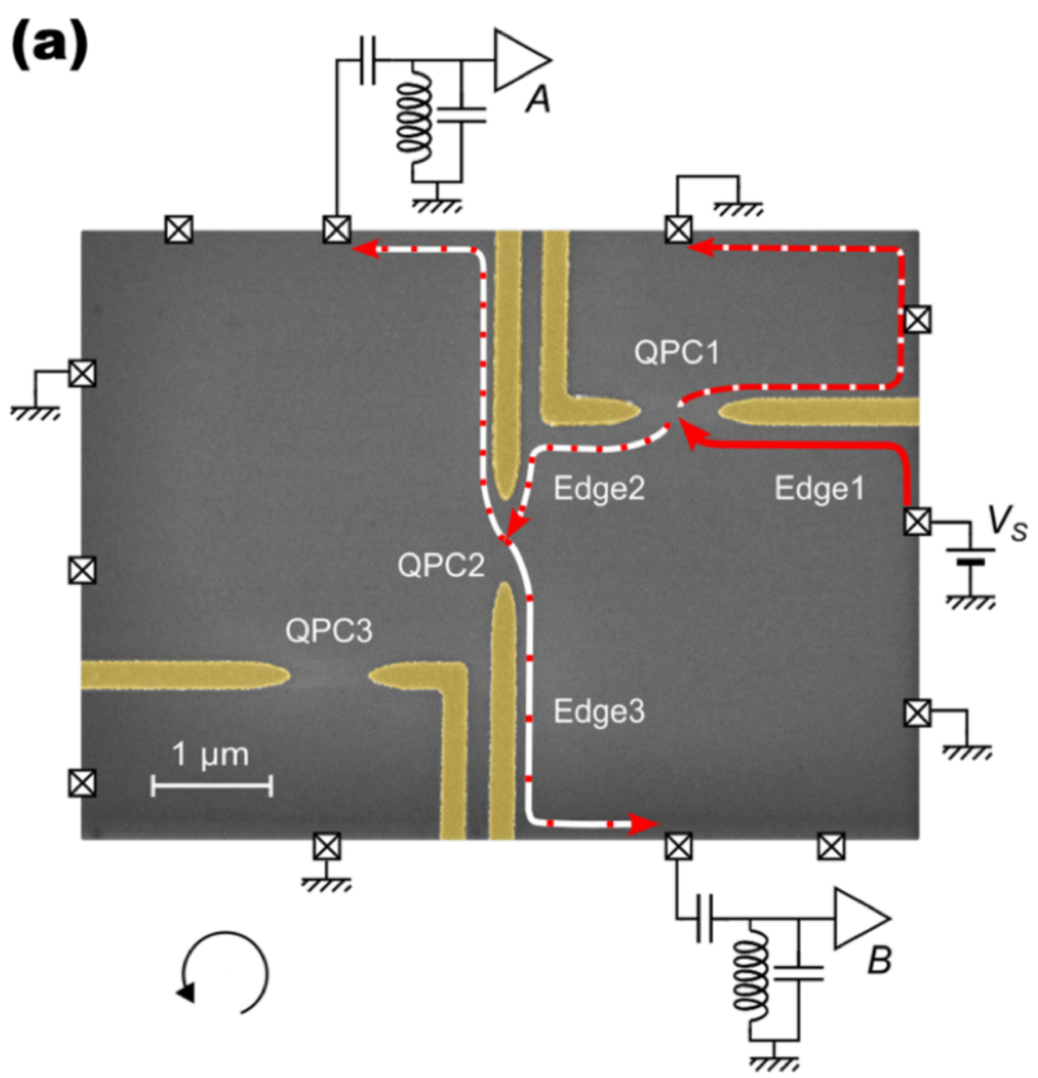

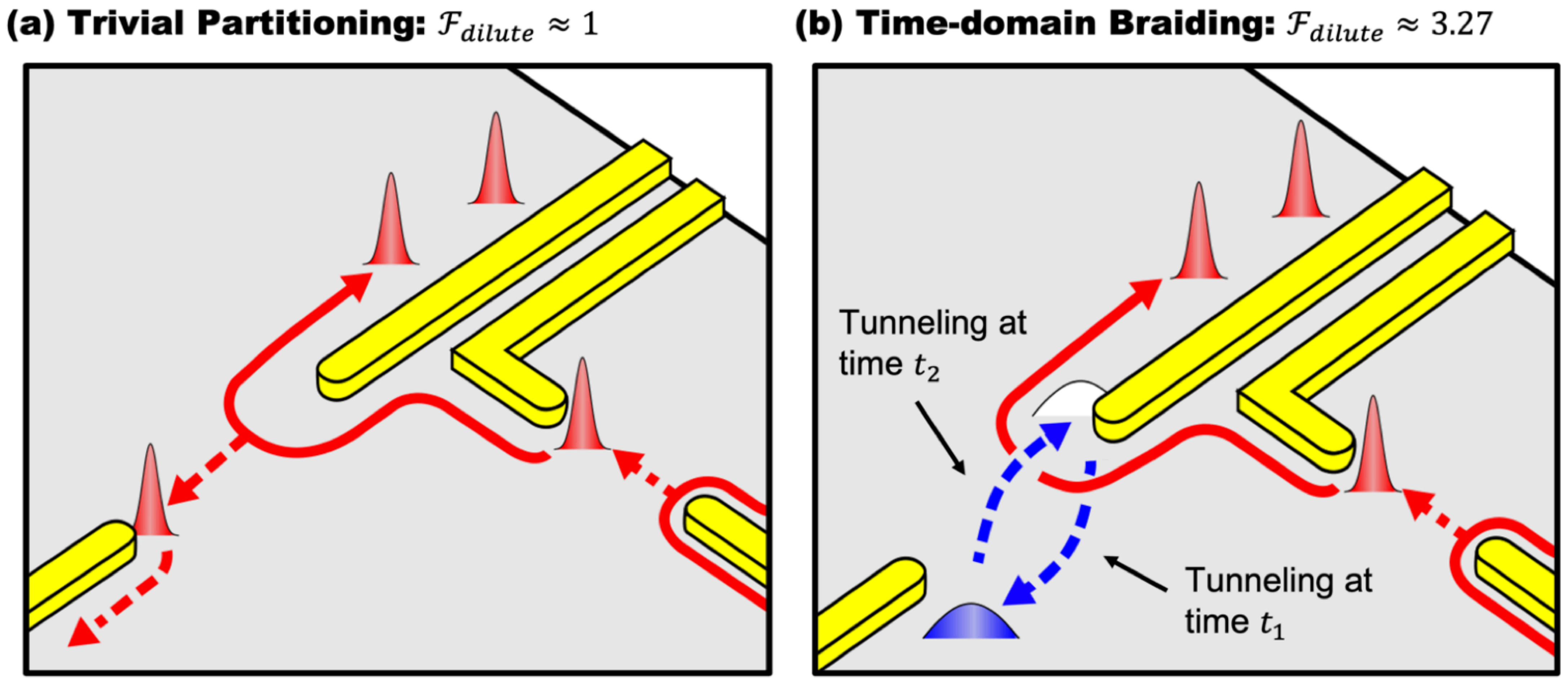

Trivial partitioning process of a highly diluted anionic beam: subdominant contribution to the observables.

More dominant process: time-domain braiding of the anyons.

The anyon that tunnels between Edge2 and Edge3 at time $t1$,, leaving a hole behind (on Edge2). This anyon tunnels back at time $t2$(and is 'pair-annihilated' with the hole. These probabilistic events of the particle-hole excitation and recombination form a loop in the time-domain. The time-domain loop of the thermal anyon in QPC2 braids with the anyons in the diluted beam that arrive at QPC2 during the time interval ($t1 - t2$).

Average braiding phase in the time-domain braiding process:

$$\langle e^{2ik\theta} \rangle_{\text{binomial}} = \sum_{k=0}^{n} P_k \, e^{2ik\theta} = \left(1 - R_{\text{QPC1}} + R_{\text{QPC1}} e^{2i\theta}\right)^n$$

$$P_k = \frac{n!}{k!(n-k)!} (R_{QPC1})^k (1 - R_{QPC1})^{n-k}$$

the probability for k anyons being reflected by QPC1 with reflection probability R_{QPC1}

$$\langle e^{2ik\theta} \rangle_{\text{binomial}} = 1$$ for fermions ($\theta = \pi$) and bosons ($\theta = 0$)

Lee, June-Young M., et al. "Partitioning of diluted anyons reveals their braiding statistics." *Nature* (2023): 1-5.

- An inter-channel distribution of EMPs at strong coupling to split electrons into fractional charges on the filling factor $\nu = 2$ IQH

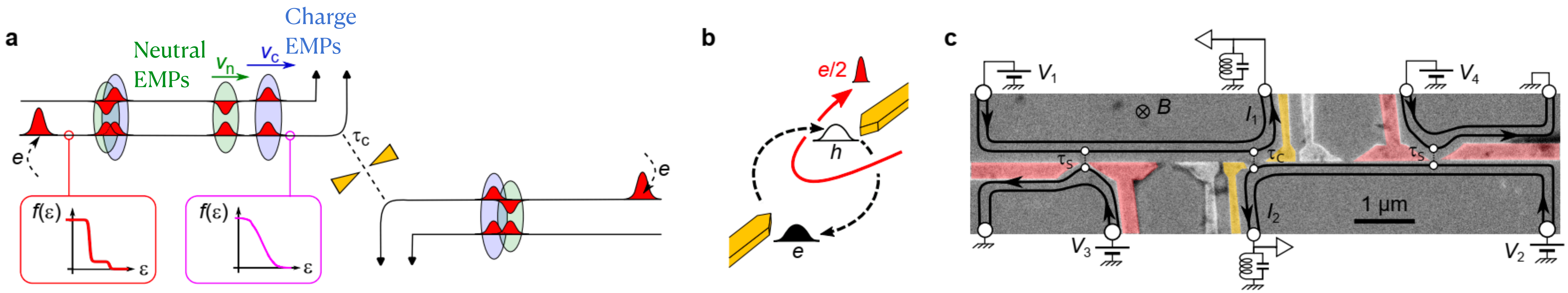

Figure 1. Experimental setup. a, In the presence of two strongly coupled quantum Hall channels at $\nu = 2$, tunneling electrons e (individual red wave-packets) progressively split into two pairs (circled). The fast 'charge' pair (blue background) consists of two co-propagating $e/2$ wave-packets, one in each channel, whereas the slow 'neutral' pair (green background) consists of opposite $\pm e/2$ charges. The fractionalized $e/2$ charges propagate toward a central QPC (yellow split gates) of transmission τ_c, used to investigate their quantum statistics from the outgoing current cross-correlations. The strong coupling regime and the degree of fractionalization at the level of the central QPC are established separately through the evolution of the electron energy distribution function $f(\varepsilon)$ from a non-equilibrium double step (red inset) to a smoother function (magenta inset). **b,** Illustration of the time-braiding mechanism, whereby an impinging fractionalized $e/2$ charge (red) braids with an electron-hole pair (black) spontaneously excited at the central QPC. **c,** E-beam micrograph of the sample. The two copropagating edge channels are drawn as black lines with arrows indicating the chirality. The aluminum gates used to form the QPCs by field effect are highlighted in false colors (sources in red, central analyzer in yellow). A negative voltage is applied to the non-colored gates to reflect the edge channels at all times. Tunneling at the sources is controlled by the applied dc voltages $V_{1,2,3,4}$ and through their gate-controlled transmission probability τ_S.

- Verification of the electrons' fractionalisation

$$f_{\text{inj}}(\varepsilon) = \tau_{\text{s}} f_{\text{FD}}(\varepsilon + eV_{\text{s}}/2) + (1 - \tau_{\text{s}}) f_{\text{FD}}(\varepsilon - eV_{\text{s}}/2),$$

τ_s: the transmission probability of outer channel electrons across the source QPC

The probed out-of-equilibrium electron energy distributions f displayed in are computed from the measured S12 (inset) using

$$f(\varepsilon = eV_{\text{p}}) \equiv \frac{1}{2}\left(1 + \frac{h}{2e^2\, \tau_{\text{c}}(1-\tau_{\text{c}})} \frac{\partial S_{12}(V_{\text{p}})}{e \partial V_{\text{p}}}\right)$$

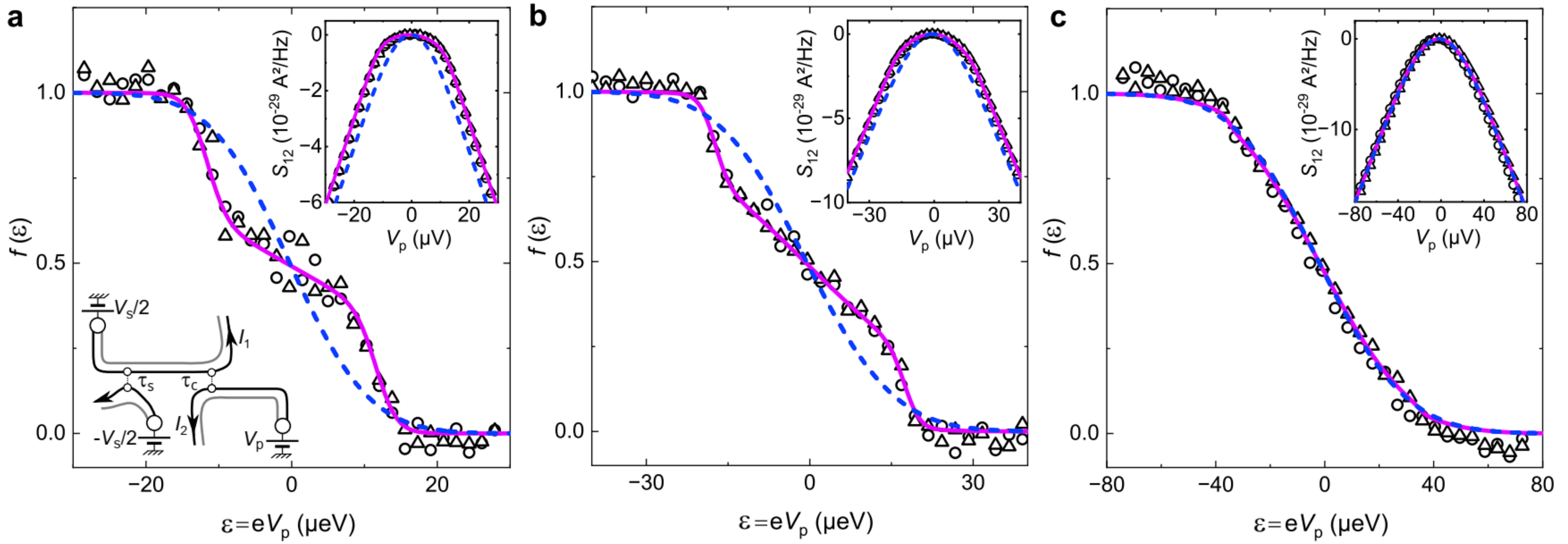

Figure 2. Spectroscopy of the electron energy distribution $f(\varepsilon)$. The shape of $f(\varepsilon)$ reflects the inter-channel coupling regime and informs on the conditions for a complete charge fractionalization at the central QPC. One source is voltage biased at V_s, here with $\tau_s \approx 0.5$, and the same probe voltage V_p is applied across the other one (see schematic in **a**). Circles and triangles show data points with the voltage biased source QPC on the left and right side, respectively. Purple continuous lines and blue dashed lines represent exact theoretical predictions in the strong coupling regime for a time delay between charge and neutral pairs of $\delta t = 64$ ps and ∞, respectively (see Supplementary Information). Insets: Cross-correlations S_{12} versus probe voltage V_p. Main panels: $f(\varepsilon)$ obtained by differentiation of S_{12}, see Eq. (1) with $\tau_c \simeq 0.5$. **a,b,c**: Data and theory at $T \simeq 11$ mK for a source voltage $V_s = 23$ μV, 35 μV, and 70 μV, respectively.

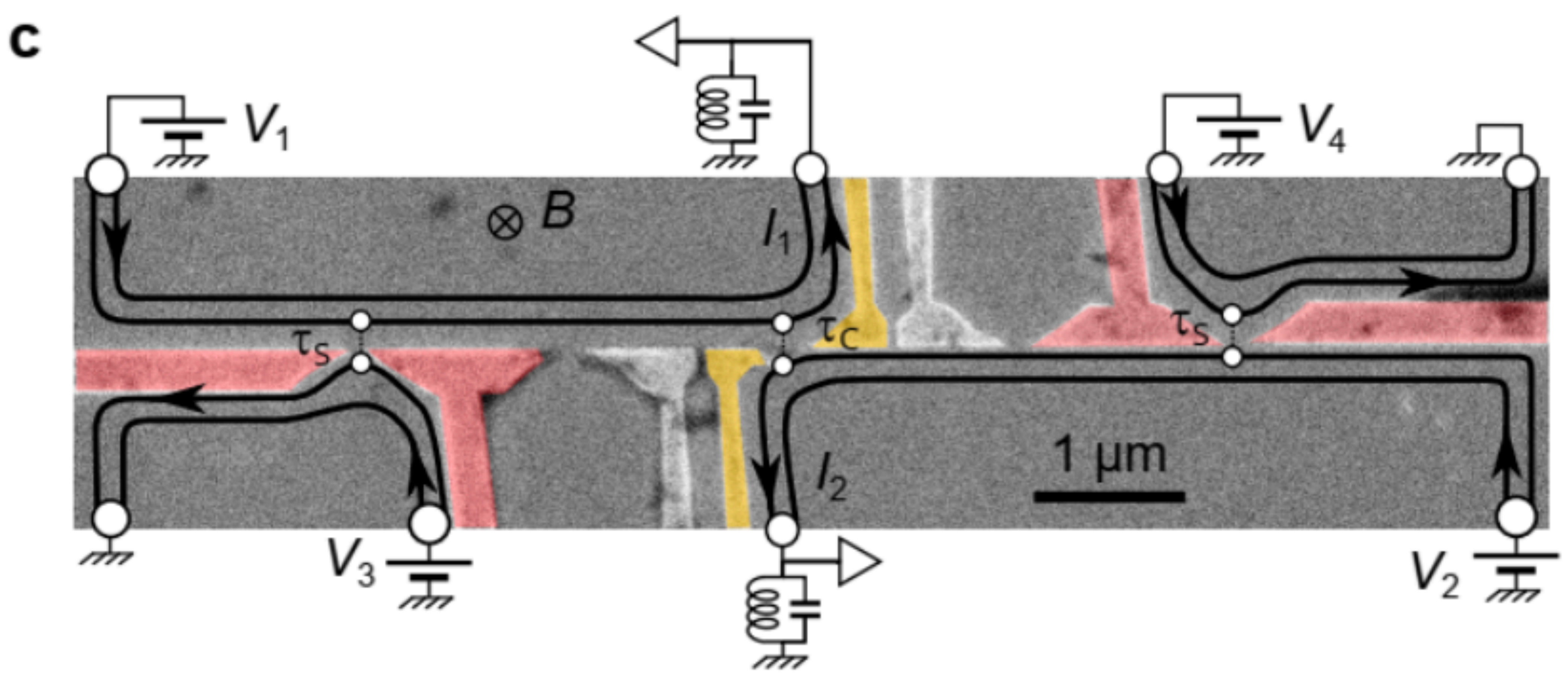

This section	Elsewhere
T_1	τ_s
T_2	τ_s
T_S	τ_c
bias V	bias V_s
spin up (↑) channel	inner channel
spin down (↓) channel	outer channel
1' channels (Fig. 5)	region biased by V_3 (Fig. **1**c Main text)
2' channels (Fig. 5)	region biased by V_1 (Fig. **1**c Main text)
1 channels (Fig. 5)	region biased by V_2 (Fig. **1**c Main text)
2 channels (Fig. 5)	region biased by V_4 (Fig. **1**c Main text)

The noise between two channels is defined as: e.g.

$$S_{1_\downarrow 2'_\downarrow}(V) = 2\int_{-\infty}^{\infty} dt \, \langle \delta\hat{I}_{1_\downarrow}(x,t)\delta\hat{I}_{2'_\downarrow}(x,0)\rangle$$

$$\delta\hat{I}_{\eta s}(x,t) = \hat{I}^H_{\eta s}(x,t) - \langle \hat{I}^H_{\eta s}(x,t)\rangle$$

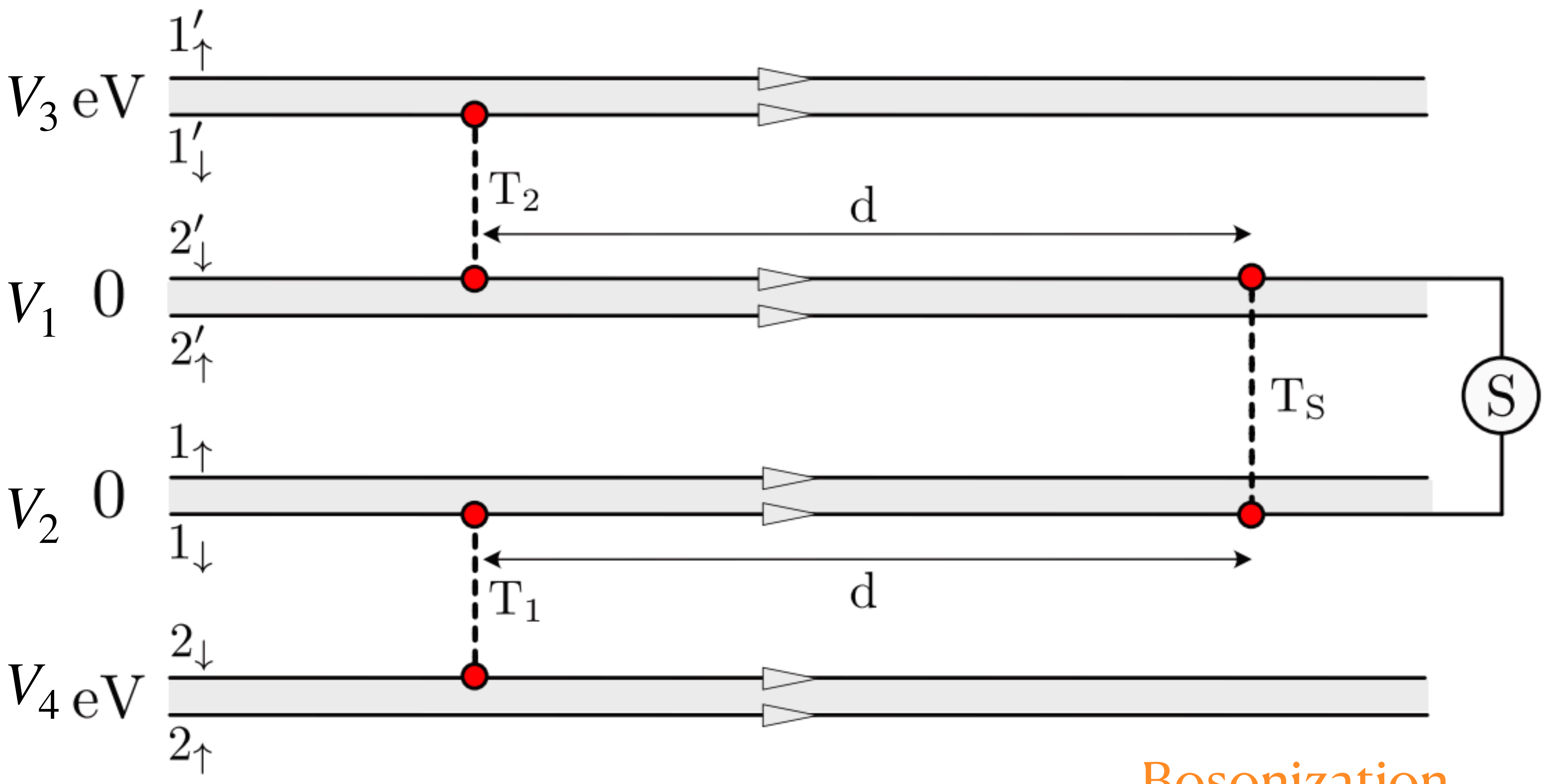

In the non-interacting case:

$$S^{(0)}_{1_\downarrow 2'_\downarrow}(V) = -2\left(\frac{e^2}{2\pi\hbar}\right) T_s R_s (T_1 - T_2)^2 |eV|$$

The QPCs 1,2 and S are described using standard tunneling Hamiltonian with corresponding transmission amplitudes v_1, v_2, v_S

Bosonization

Refermionization

(In SI)

$$\hat{H} = -i\hbar v_F \sum_{\eta=1,1',2,2',s=\uparrow,\downarrow} \int_{-\infty}^{\infty} dx \; \hat{\Psi}^\dagger_{\eta s}(x)\partial_x \hat{\Psi}_{\eta s}(x) + 2\pi\hbar g \sum_{\eta=1,1',2,2'} \int_{-\infty}^{\infty} \hat{\rho}_{\eta\uparrow}(x)\hat{\rho}_{\eta\downarrow}(x)dx$$

$$+ [v_1 \hat{\Psi}^\dagger_{1\downarrow}(0)\hat{\Psi}_{2\downarrow}(0) + v_2 \hat{\Psi}^\dagger_{1'\downarrow}(0)\hat{\Psi}_{2'\downarrow}(0) + v_s \hat{\Psi}^\dagger_{2'\downarrow}(d)\hat{\Psi}_{1\downarrow}(d) + h.c.].$$

- Negative cross-correlation signature of anyon statistics

Generalised Fano factor:

$$P \equiv \frac{S_{12}}{\tau_c(1-\tau_c)S_\Sigma},$$

τ_c is the analyzer transmission, S_Σ is the sum of the current noises emitted from the two source QPCs

Non-zero P: a qualitative signature of an unconventional braiding statistics

In the dilute limit ($\tau_s \ll 1$):

$$P \simeq \frac{\sin^2\theta}{\theta^2}\ln\tau_s,$$

Perturbative analysis, -1.2

In braiding between incident fractional charges e/2 and electron-hole pairs, θ = π/2

$$P = \frac{4}{\pi^2}\ln\tau_s + \frac{4}{\pi^2}\tau_s\ln\tau_s - 0.3\tau_s + 0.943.$$

Non-perturbative treatment, -0.35

Shot noise prediction for

$$S_\Sigma = 2\frac{e^2}{h}\sum_{i=L,R}\tau_i(1-\tau_i)eV_s\left[\coth\left(\frac{eV_s}{2k_BT}\right) - \frac{2k_BT}{eV_s}\right], \quad (3)$$

with $T = 11$ mK and $\tau_{L(R)}$ the measured dc transmission of the left (right) source shown in the top inset.

c

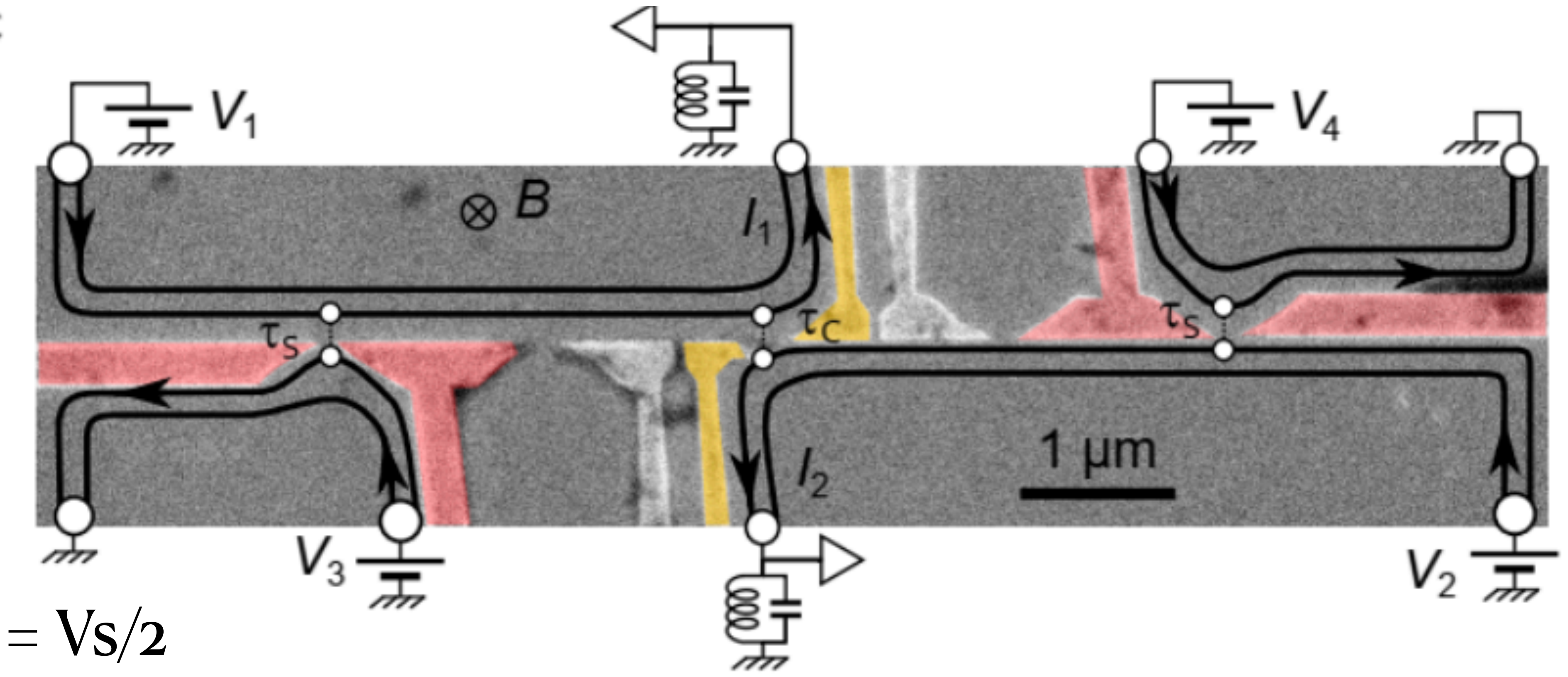

V1,2 = −V3,4 = Vs/2

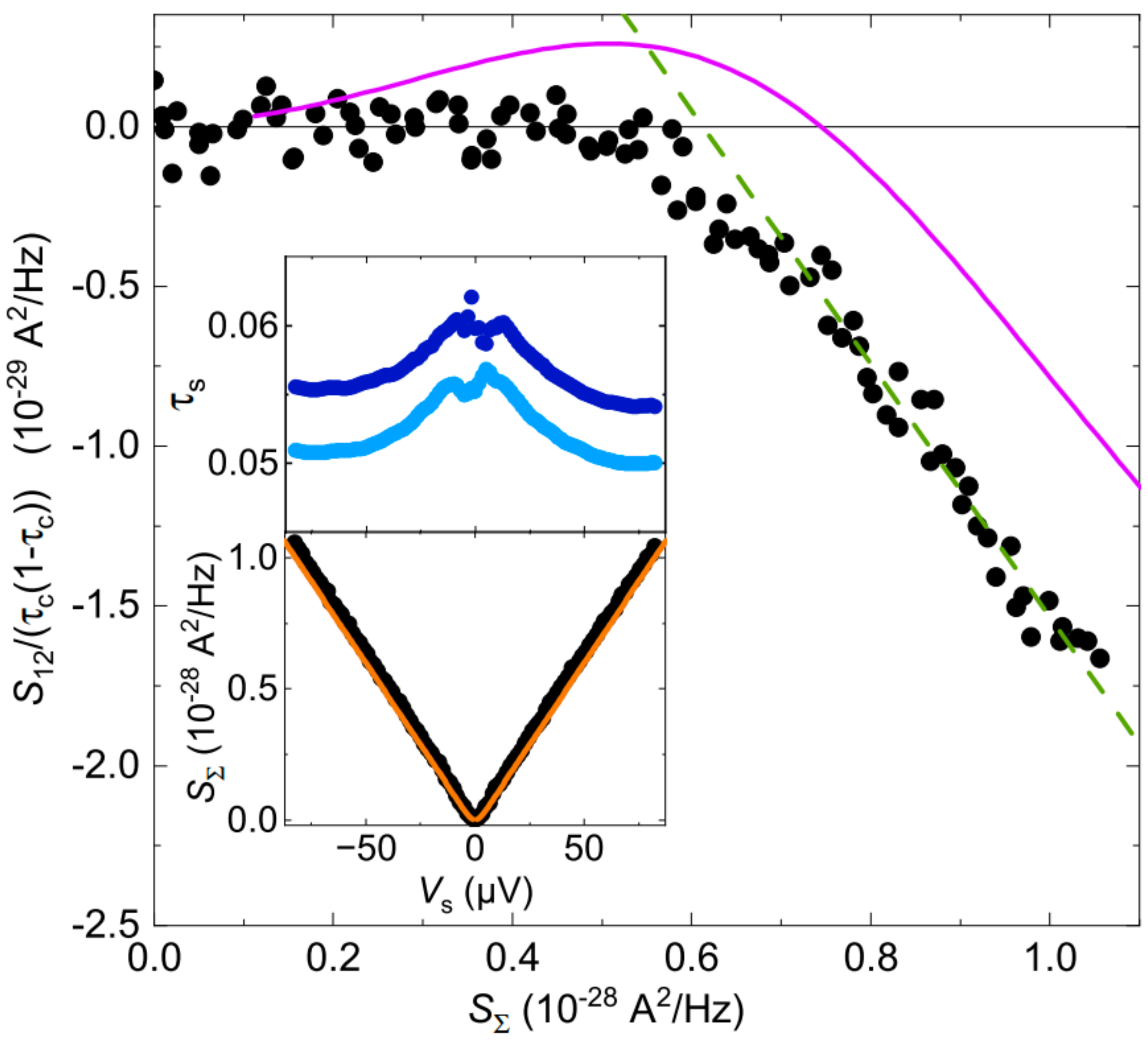

Figure 3. Cross-correlation signature of fractional statistics with symmetric dilute beams. Measured excess shot noise $S_{12}/(\tau_c(1-\tau_c))$ as a function of source shot noise S_Σ for a small source QPC transmission $\tau_s = 0.05$. The purple continuous line displays the strong inter-channel coupling prediction for $\delta t = 64$ ps. The dashed green line denotes the slope, i.e., the Fano factor (see Main text), yielding $P \simeq -0.38$. Top inset: Measured left/right source QPC dc transmission as a function of bias voltage, shown in light/dark blue, respectively. Bottom inset: Sum of sources' shot noise S_Σ vs source bias voltage V_s. The orange line displays Eq. (3) with $T = 11$ mK, the independently measured temperature.

- evidence of the underlying anyonic mechanism is provided from the effect of the dilution of the quasiparticle beam

Outer edge channel, 2 $e/2$

inner edge channel, $\pm e/2$

Outer channels are fully transmitted

Away from the dilute limits, an increasing importance of the positive contribution from the noise generated at the sources with respect to the noise generated at the analyzer involving the emergence of mechanisms other than time braiding (such as collisions)

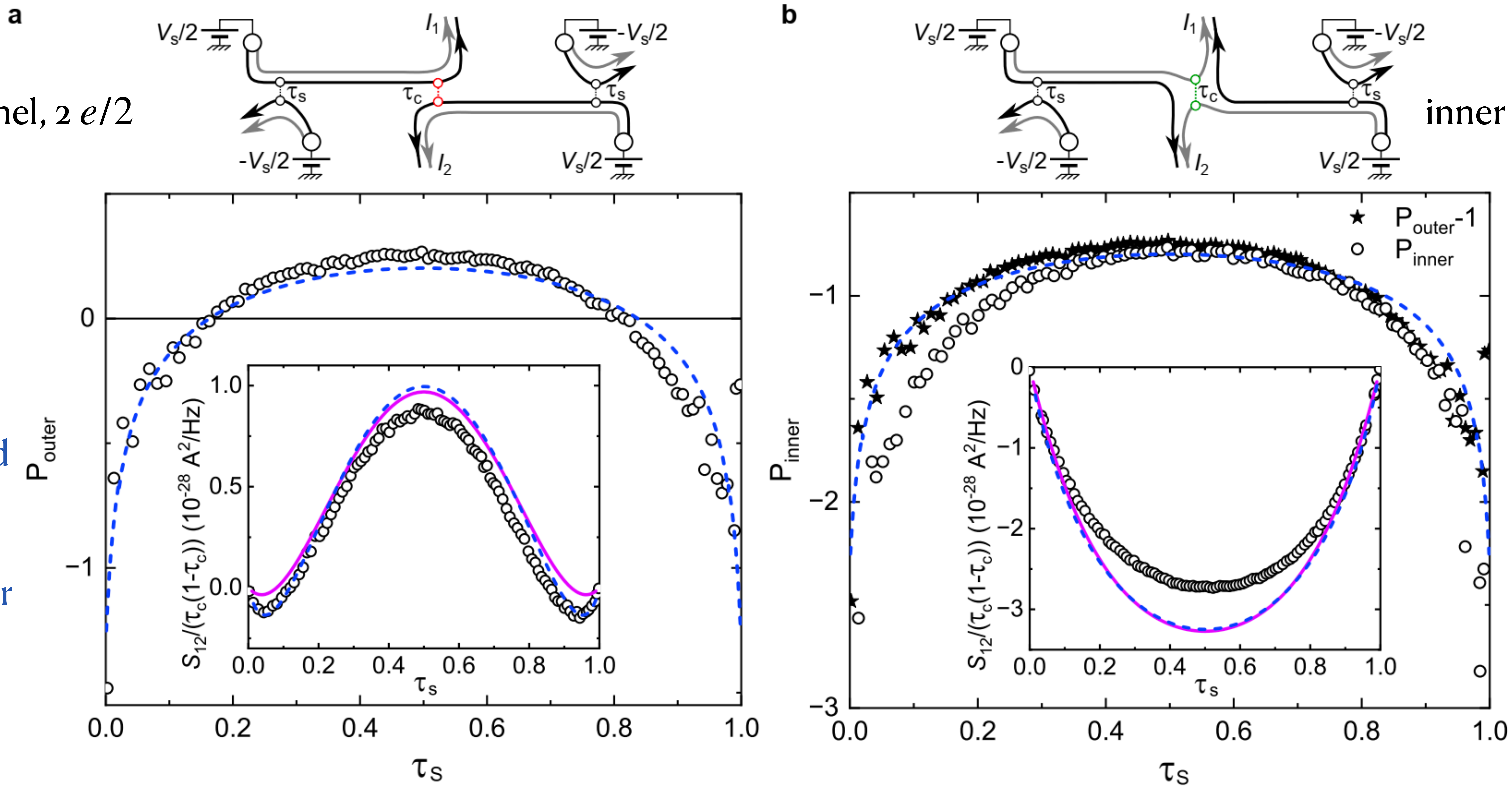

Figure 4. **Cross-correlations vs dilution** of symmetric beams. Main panels and insets show, respectively, the generalized Fano factor P and the renormalized cross-correlations $S_{12}(V_s = 70\ \mu V)/(\tau_c(1-\tau_c))$ vs the outer edge channel transmission τ_s of the symmetric source QPCs. Symbols are data points. Blue lines are high bias/long δt predictions. Purple lines are $S_{12}(V_s = 70\ \mu V)/(\tau_c(1-\tau_c))$ predictions at $\delta t = 64$ ps. **a**, The cross-correlation signal and corresponding P_{outer} (open circles) are measured by partially transmitting at the central QPC ($\tau_c \approx 0.5$) the same outer edge channel (black) where electrons are tunneling at the sources (see schematics). This is the standard 'collider' configuration. **b**, The cross-correlation signal and corresponding P_{inner} are obtained by setting the central QPC to partially transmit ($\tau_c \approx 0.5$) the inner edge channel (grey), whereas electrons are tunneling into the outer edge channel at the sources (see schematic). In this particular configuration, the source shot noise does not directly contribute to the cross-correlation signal. Filled symbols in the main panel display $P_{outer} - 1$, with P_{outer} the data in (**a**) and -1 corresponding to the subtraction of the source shot noise.

Conclusion

Advanced and time-resolved quantum manipulations of anyons are made possible by the large quantum coherence along the integer quantum Hall edge and the robustness of the incompressible bulk. By tailoring single-quasiparticle wave-packets, for example with driven ohmic contacts, a vast range of fractional anyons of arbitrary exchange phase becomes available along the integer quantum Hall edges, well beyond the odd fractions of π of Laughlin quasiparticles encountered in the fractional quantum Hall regime.